Accepted Manuscript

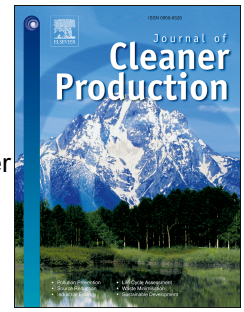

Application of response surface methodology to optimize direct alcohol fuel cell power density for greener energy production

Kanin Charoen, Chaiwat Prapainainar, Panitas Sureeyatanapas, Theeraporn Suwannaphisit, Kanchaporn Wongamornpitak, Paisan Kongkachuichay, Stuart M. Holmes, Paweena Prapainainar

PII: S0959-6526(16)31400-7

DOI: 10.1016/j.jclepro.2016.09.059

Reference: JCLP 8019

To appear in: *Journal of Cleaner Production*

Received Date: 15 January 2016

Revised Date: 8 September 2016

Accepted Date: 9 September 2016

Please cite this article as: Charoen K, Prapainainar C, Sureeyatanapas P, Suwannaphisit T, Wongamornpitak K, Kongkachuichay P, Holmes SM, Prapainainar P, Application of response surface methodology to optimize direct alcohol fuel cell power density for greener energy production, *Journal of Cleaner Production* (2016), doi: 10.1016/j.jclepro.2016.09.059.

Application of Response Surface Methodology to Optimize Direct Alcohol Fuel Cell Power Density for Greener Energy Production

Kanin Charoen[1], Chaiwat Prapainainar[2,3], Panitas Sureeyatanapas[4], Theeraporn Suwannaphisit[1], Kanchaporn Wongamornpitak[1], Paisan Kongkachuichay[1,5], Stuart M. Holmes[6], and Paweena Prapainainar[1,5*]

[1]*Departmentof Chemical Engineering, Faculty of Engineer, Kasetsart University, Bangkok, 10900, Thailand*

[2]*Departmentof Chemical Engineering, Faculty of Engineer, KMUTNB, Bangkok, 10800, Thailand*

[3]*Research and Development Centre for Chemical Engineering Unit Operation and Catalyst Design, King Mongkut's University of Technology North Bangkok, Bangkok 10800, Thailand*

[4]*Department of Industrial Engineering, Faculty of Engineering, Khon Kaen University, Khon Khan 40000, Thailand*

[5]*NANOTEC Center for Nanoscale Materials Design for Green Nanotechnology and Center for Advanced Studies in Nanotechnology for Chemical, Food and Agricultural Industries, Kasetsart University, Bangkok, 10900, Thailand*

[6]*School of Chemical Engineering and Analytical Science, The University of Manchester, Manchester M13 9PL, UK*

*Corresponding author: fengpwn@ku.ac.th

1. Abstract

Energy production from direct alcohol fuel cells depends strongly on the operating conditions. In this research, the aim was to find the best conditions of direct methanol fuel cells (DMFC) and direct ethanol fuel cells (DEFC) to obtain the maximum power density with the response surface method using Program Design Expert 7.0.0.

Three related independent variables, including operating temperature in the range of 30-70°C, alcohol flow rate in the range of 5-50 ml/min, and alcohol concentration in the range of 0.5-3 M, were covered. Nafion117 was used as an electrolyte and Pt-Ru and Pt were used as catalysts in anode and cathode, respectively. The effect of those variables on the maximum power density was illustrated in the form of quadratic models which predicted the appropriate operating conditions. The Nafion membrane was modified by adding mordenite (MOR) to improve its alcohol permeability. The result from response revealed that the higher operating temperatures and higher alcohol concentrations led to an increase in maximum power density, in both the DMFC and DEFC. The DMFC had a higher maximum power density and greater current than the DEFC had. This was because methanol was easier to oxidize than ethanol In addition, it was found that the MOR content of 1.47 wt% in the Nafion composite membrane reduced the alcohol permeability and resulted in a higher power density. Therefore, the model suggested the optimum conditions to produce greener energy (less resource use with high energy produced).

Keywords: Response surface method; greener energy production; direct alcohol fuel cell; maximum power density; Nafion-composite membrane

2. Introduction

The main fuel source for the world up to now has been fossil fuels consisting of coal, petroleum, and natural gas, which are expensive and limited in supply. The combustion of fuels causes air pollution that affects human health and increased carbon dioxide levels which causes global warming (Lecksiwilai et al.; Permpool et al.). Fuel cells as a clean alternative energy source have been developed continuously to reduce the consumption of fossil fuels. Fuel cells can be used both in automotive electronics and industrial applications. Electricity production from fuel cells is highly efficient and environmentally friendly compared to that from other types of energy (Andreasen and Sovacool, 2015). Proton Exchange Membrane Fuel Cells (PEMFC) are among the most

suitable to be used in automotive applications, because they provide high power density and can be operated at low temperatures (Hall and Kerr, 2003). However, the problems of hydrogen gas are the relatively high cost, low energy density, and high flammability. Direct alcohol fuel cells (DAFC) has been developed later. Methanol or ethanol can be used as fuels which are cheap and easy to find. Direct methanol fuel cells (DMFC) can be operated at relatively low temperatures and are thus suitable to be used as a power source in portable electronics devices (Calabriso et al., 2015). Direct ethanol fuel cells (DEFC) uses ethanol as a fuel. They are suitable for agricultural economics as ethanol can be derived from the fermentation process of agricultural products and waste materials such as sugarcane, corn, molasses, and cassava. The working principles of DMFC and DEFC are similar. Fuel is fed into the fuel cell sack and the oxidation reaction takes place at the catalyst surface at the anode and the reduction occurs at the cathode. The reactions are shown in equations (1)-(3) for DMFC (Mallick et al., 2015; Mudiraj et al., 2015) and equations (4)-(6) for DEFC (Abdullah et al., 2015; Badwal et al., 2015).

Anode :	$CH_3OH + H_2O$	$\longrightarrow$	$CO_2 + 6H^+ + 6e^-$	(1)
Cathode :	$3/2O_2 + 6H^+ + 6e^-$	$\longrightarrow$	$3H_2O$	(2)
Overall reaction :	$CH_3OH + 3/2\ O_2$	$\longrightarrow$	$CO_2 + 2H_2O$	(3)
Anode :	$C_2H_5OH + 3H_2O$	$\longrightarrow$	$2CO_2 + 12H^+ + 12e^-$	(4)
Cathode :	$3O_2 + 12H^+ + 12e^-$	$\longrightarrow$	$6H_2O$	(5)
Overall reaction :	$C_2H_5OH + 3O_2$	$\longrightarrow$	$2CO_2 + 6H_2O$	(6)

In the reaction of DMFC, six electrons are released by the oxidation reaction at the anode transfer to the cathode by an external circuit providing power to the connected devices. Protons (H^+) diffuse through the proton exchange membrane, mostly Nafion117,

from the anode to the cathode then react with electrons travelling from the electronic device to the cathode and oxygen gas in the fed air. The process releases water and carbon dioxide as by-products. In case of DEFC, twelve electrons are released which tend to provide higher power than DMFC. However, it also produces two mole of carbon dioxide per one mole of alcohol, which is twice that from DMFC. It seems to impact negatively on the environment. However, the released CO_2 does not impact the environment, because the ethanol is derived from fermentation of agricultural crops and the plants grow by photosynthesis process which consumes CO_2. Thus, it can be seen that the produced CO_2 can be circulated to the plants. Hence, it neither contributes to global warming nor increases carbon dioxide in the atmosphere. It was concluded that DEFC is one of alternative environmentally friendly sources of energy.

At present, DAFCs are to be improved in several areas for better performance, such as catalysts at the electrodes (Cheng et al., 2015; Jurzinsky et al., 2015; Li et al., 2015), design of flow field (Wu et al., 2016), and proton-exchange membrane (Sha Wang et al., 2015). Nafion is a good candidate for the proton exchange membrane in DAFC because it has a lot of superior properties such as high ionic conductivity (Yoonoo et al., 2011), as well as high thermal and chemical stabilities. It is able to absorb a large amount of water due to the hydrophilic property of the sulfonated groups. H^+ can split from the sulfonic group and provides the proton conduction. However, Nafion membrane has problems with a high degree of alcohol permeability that causes the reduction of the DAFCs performance. This research also aimed to improve the alcohol resistance by adding mordenite (MOR), which is an inorganic filler to form Nafion composite membranes. MOR has hydrophilic and molecular sieves properties. It preferentially adsorbs water over alcohol which can obstruct the flow of alcohol but allows water to pass through the membrane with good proton transport (Yoonoo et al., 2011). It also has additional features such as stability in acidic environments, high thermal stability and high tolerance of alcohol environments which are advantages for DAFC. (Prapainainar et al., 2015)

In this paper, the results are divided into 3 parts. The first and second parts cover the optimization of the operating conditions of DMFC and DEFC by using the response Surface Methodology (RSM) with the central composite design (CCD) method. The RSM technique is a process of mathematical and statistical calculation–useful for analyzing the effects of several independent variables in order to determine variable settings that optimize the response value (Alshehria et al., 2015; Okur et al., 2014). CCD is generally used when curvature in the response surface is suspected but the number of trials in an experiment needs to be minimized or resources are limited. The Design Expert version 7.0 software program was used to design the experiment to determine the effect of three operating variables on the performance of DAFC. The studied variables were operating temperature in the range of 30-70°C, alcohol flow rate in the range of 5-50 ml/min, and alcohol concentration in the range of 0.5-3 M. The third part was to find the optimum MOR content in Nafion-composite membrane from 0 wt% up to 10 wt%. The interested response for every part was the power density of the fuel cells.

3. Methodology

3.1 The central composite design

In the first part of our experiment, the operating conditions to obtain the highest power density of DMFC and DEFC were optimized using CCD, which was a method in RSM (Zainoodin et al., 2015). Three variable - alcohol flow rate, alcohol concentration, and operating temperature - were included in the predicted model. According to the design, the trial was derived randomly into 30 different experimental conditions for each type of fuel cell, with 4 replication runs and 2 runs at the center point. The results from the performance test were fitted to a second-order polynomial model, as shown in equation (7)

$$y = \beta_0 + \beta_1 A + \beta_2 B + \beta_3 C + \beta_{12} AB + \beta_{13} AC + \beta_{23} BC + \beta_{11} A^2 + \beta_{22} B^2 + \beta_{33} C^2 \qquad (7)$$

where y is the response or dependent variable. A, B and C are the independent variables of this study (fuel flow rate, fuel concentration, and operating temperature, respectively). β_0 is the regression coefficient at the center point. β_1, β_2 and β_3 are the linear coefficients. β_{12}, β_{13} and β_{23} are the quadratic coefficients. β_{11}, β_{22} and β_{33} are the second-order interaction coefficient.

The values of these coefficients and the optimum levels were calculated. The obtained equation was used to explain the relationship between the response and the variables. How well the data from the experiment match with our statistical model was expressed as the coefficient of determination, R^2. The maximum power density of the single cell performance test was considered as the response. Finally, the optimum conditions could be generated at the maximum power density for each fuel cell. For the final part of the experiment, we aimed to improve the performance of the membrane with various MOR contents to find the optimum MOR content in the membrane. At this stage, the experiment was done on DMFC because it provided the highest maximum power density of the previous sections. The historical data with 100 conditions were applied with three variables: methanol concentration of 1-8 M, operating temperature of 30-70°C, and MOR content of 0 – 10 wt%.

3.2 Membrane electrode assembly fabrication

For MEA fabrication, 60 wt% Pt-Ru alloy on Vulcan XC-72 from E-Tek was used as an anode electrode and 60 wt% Pt on Vulcan XC- 72 carbon from E-TEK was used as a cathode electrode. The metal loading in each electrode was 1 mg Pt/cm^2 based on the total metal weight. The dimensions of the electrode was 45x45 mm^2 and the total surface area was 20.25 cm^2. Nafion117 was purchased from ETEK and pretreated by boiling in 5% H_2O_2 for 30 min and in 1 M H_2SO_4 for 30 min. After that, it was washed in boiling DI water for 10 min for 3 rounds. MOR for the experiment in section 4.3 was purchased from Zeolyst International (CBV10A). MEA was fabricated with the spray-

coating method. The catalyst was sprayed on top of the gas diffusion layer, forming catalytic coated backings. After that, the catalytic coated backings and pre-treated membrane electrolytes were assembled together by hot-pressing at 135 °C with pressure of 50 kg/cm^2 for 3 min to obtain MEA.

3.3 Single cell performance test setup

The diagram of a single cell performance test is shown in Figure 1. The prepared alcohol solution was stored in a storage tank (fuel tank) connected to a peristaltic pump (Lead fluid BT301L). The pump was used to control the fuel flow rate at 5 ml/min and delivered to the fuel cell at the anode. An external power supply (GWInstek GPR-30600) was used to control the current flowing through the cell. Air zero (oxygen), purchased from Praxair Inc. was connected to the fuel cell at the cathode. A flow meter (Influx B9HP-A16) was used to control the air flow rate equal to 1000 ml/min. The operating temperature of the fuel cell was controlled by a temperature controller together with a thermocouple and electric heaters. The voltage output was measured with a digital multimeter (Evertech YF-78-TAIWAN).

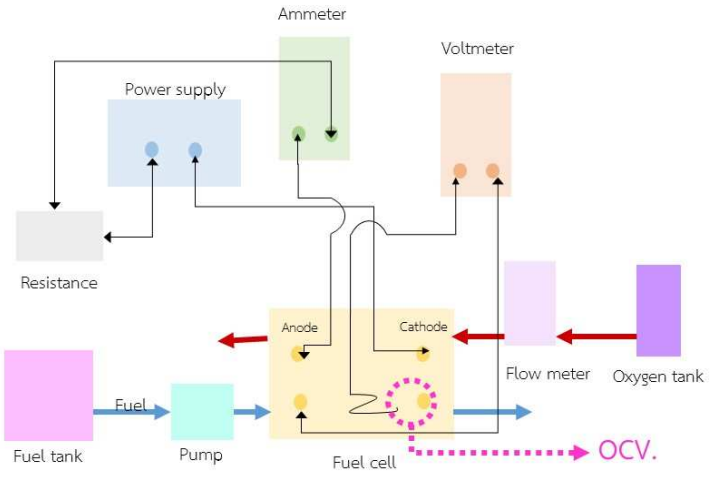

Figure 1 Fuel cell experimental set up.

3.4 Measurements and calculations

The voltage output was measured at steady state with a digital multimetre (Evertech YF-78-TAIWAN). The data was recorded at different current values. The corresponding current was based on the equation $I=V/R_{ext}$, where I is the current (mA), V is the voltage (mV) and R_{ext} is the external resistance (Ω). The power density of the fuel cell was obtained from the equation $P_{den}=I_{den}V$, where I_{den} is the current density which was calculated from the current (I) divided by the surface area of the electrode (20.25 cm^2). The polarization curve was obtained by plotting between the voltage and the current density. The maximum power density at each operating condition was calculated and recorded for further analysis using RSM.

4. Results and Discussion

The experiment and result were divided into 3 sections. The first and the second sections were the optimization of DMFC and DEFC, respectively. The third section was the optimization of the MOR content in the composite membrane on power density

4.1 The optimization of direct methanol fuel cell

The first part of this study was to find the optimum condition of DMFC. The conditions designed with Design Expert 7.0 software program and the maximum power density of the DMFC single cell performance test at different operating conditions are shown in Table 1. The examples of polarization curve of DMFC operated at lower and upper bounds of variables in the optimization were shown in Figure S1 and Figure S2 (in supplementary data). The result from RSM analysis by using the analysis of variance (ANOVA) is provided in Table 2. The prediction model is shown in equation (8). The ANOVA results of the second-order polynomial model were used to illustrate the

response of power density in the experiment. It should be noted that the effect of each independent variable on the response was the combination of coefficients with variable values. That cannot be investigated by using one factor at a time method.

Table 1 Operating conditions of DMFC obtained from Design Expert 7.0 and power density from experiment.

Run	Methanol flow rate (mL/min)	Methanol conc. (M.)	Operating temperature (°C)	Power Density (mW/cm^2)
1	54.5	1.75	50	4.56
2	27.5	1.75	26	3.06
3	50.0	3.00	70	1.85
4	50.0	0.50	30	3.28
5	0.5	1.75	50	5.50
6	27.5	1.75	26	3.26
7	54.5	1.75	50	4.33
8	27.5	3.25	50	4.00
9	0.5	1.75	50	5.33
10	27.5	0.25	50	6.37
11	50.0	3.00	30	1.16
12	27.5	1.75	74	5.53
13	5.0	0.50	30	2.42
14	50.0	0.50	30	3.16
15	50.0	0.50	70	6.50
16	50.0	0.50	70	6.15
17	5.0	3.00	30	1.40
18	27.5	1.75	74	5.53
19	50.0	3.00	70	1.78
20	5.0	0.50	70	6.22
21	27.5	1.75	50	4.63
22	27.5	1.75	50	4.53
23	27.5	0.25	50	6.64
24	5.0	3.00	70	2.52
25	5.0	0.50	30	2.44
26	5.0	3.00	30	1.38
27	50.0	3.00	30	1.08
28	5.0	0.50	70	6.07
29	27.5	3.25	50	3.79
30	5.0	3.00	70	2.44

Table 2 ANOVA results of DMFC for the response obtained from quadratic equation of Design Expert 7.0.

Source	Sum of Squares	df	Mean Square	F Value	p-value Prob> F
Model	88.90	9	9.88	37.45	< 0.0001
A-Methanol flow rate	0.23	1	0.23	0.89	0.3571
B-Methanol concentration	38.37	1	38.37	145.48	< 0.0001
C-Cell temperature	24.10	1	24.10	91.36	< 0.0001
AB	0.91	1	0.91	3.44	0.0784
AC	0.25	1	0.25	0.96	0.3395
BC	6.34	1	6.34	24.03	< 0.0001
A^2	4.50	1	4.50	17.04	0.0005
B^2	2.48	1	2.48	9.39	0.0061
C^2	10.92	1	10.92	41.41	< 0.0001
Residual	5.27	20	0.26		
Pure Error	0.21	15	0.014		
Cor Total	94.18	29			
Std. Dev.	0.51				
R-Squared	0.9440				

Source	Sum of Squares	df	Mean Square	F Value	p-value Prob> F
Adj R-Squared	0.9188				

4.1.1 Statistical analysis

R-Square of the second polynomial model in equation (8) was 0.9440 and the Adj R-Squared was 0.9188. R-square indicates the amount of variation in the response values that is explained by the combination of variables being considered. Here, R-Square was sufficiently high, which meant that there were sufficient data and the model was reliable enough to be used to predict the power density. However, R-Square that was slightly higher than the adjusted value implied that the model may include unnecessary variables which did not significantly influence the response.

$$\text{Power Density} = 5.64-0.10A-1.33B+1.05C-0.24AB-0.13AC-0.63BC-0.73A^2-0.54B^2-1.13C^2 \quad (8)$$

where A is methanol flow rate (ml/min), B is methanol concentration (molar), and C is operating temperature (°C).

Analysis of variance can be analyzed by the P-value from Table 2. It was found that the P-value model was less than 0.0001. It can be concluded that this model was sufficient to use, as it was less than the level of significance ($\alpha = 0.05$) (Kahveci and Taymaz, 2014). The P-value of A was equal to 0.3571, which was greater than 0.05. Thus, this indicated that the methanol flow rate did not significantly affect the power density. The P-values of the interaction effects AB and AC were also greater than the significance level, and this confirmed that the flow rate had only a tiny negligible effect on the power density. The model can become more accurate by reducing the number of non-significant terms (Taymaz et al., 2011). On the other hand, the P-values of B and C were lower than the significance level. This means the power density did significantly vary with changes in methanol concentration and operating temperature. Their interaction effect on the power density, as seen in the P-value of BC lower than 0.05, was also

significant. Generally speaking, the effect of each value on the power density depended on the value of another. The P-values of squared effects were all lower than 0.05, and this indicated that the relationships between each variable and the power density tended to follow a curved line.

Figure 2 shows the comparison between actual power density and predicted power density from the prediction model. Each point in the graph demonstrates the actual power density of the experiment that was close to the power density of the predicted value. The linear trend suggests that the actual power density had a normal distribution, which led to the conclusion that this model could sufficiently predict the response. Different colors indicated the value at each point of power density. For example, red represented the highest power density, down to blue which represented the minimum power density (Kahveci and Taymaz, 2014).

Figure 3 plots of the residual value of power density to the prediction of power density which shows the accuracy of prediction. It was calculated from the experimental value minus the predicted value. The positive value on the y-axis indicated that the predicted value was too low. On the other hand, a negative value on the y-axis indicated that the predicted value was higher than the experimental value. The data with zero distance from the x-axis indicated that the experimental results matched well with the predicted values. Figure 3 shows that each point of the experiment fluctuated slightly over the x-axis. It can be concluded that the models and experimental results were considered satisfactory (Zainoodin et al., 2015).

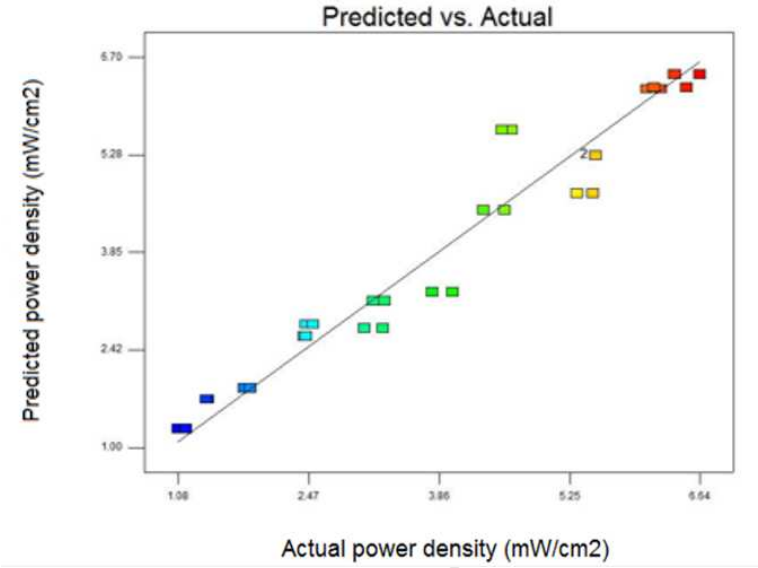

Figure 2 Maximum power density of DMFC between actual and predicted value.

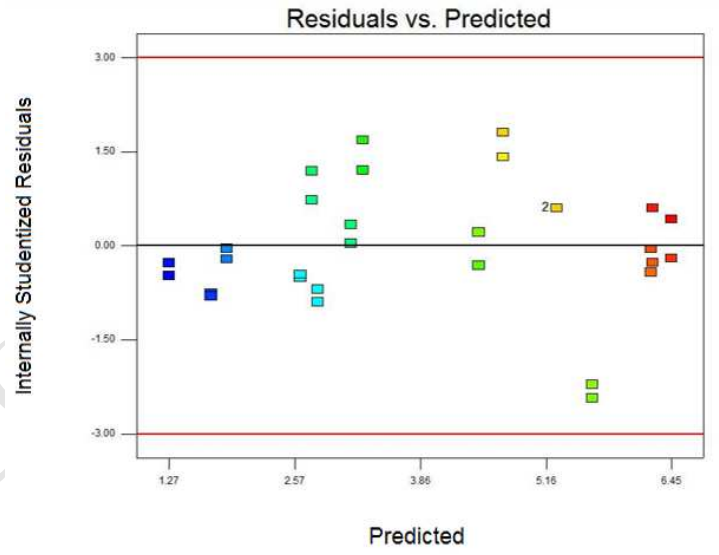

Figure 3 Residual value of power density and predicted power density of DMFC.

4.1.2 Effect of temperature

The response surface of DMFC operation from the program shown in Figure 4 was a plot between methanol concentration and operating temperature on the power density at a constant methanol flow rate of 27.50 mL/min. Considering at the same concentration of methanol, it was found that the maximum power density greatly increased as the operating temperature rose from 30°C to 70°C. This result was in agreement with the research by Chen et al. (2010). The fuel cell operating temperature greatly contributed to the efficiency of fuel cells due to the reaction rate of the methanol oxidation at the anode and oxygen reduction at the cathode were accelerated according to the Arrhenius equation (Yuan et al., 2015). Moreover, it enhanced the amount of H^+ travelling through the membrane and resulted in an increase in the electricity produced (Heysiattalab et al., 2011). Moreover, higher temperature caused the polymer backbone to expand due to softening of the fluorinated chain. This can accelerates the alcohol molecules' thermodynamic motion resulting in higher alcohol transportation rate through the membrane. As a result, a loss of the fuel at the anode side and the cross fuel through membrane can generate a mixed potential at the cathode which can negate the potential that occurs at the anode. This was why the power density increased with the declined rate at a high temperature, as seen in Figure 4. From this Figure, it was observed that the operating temperature and methanol concentrations were strongly affected the power density.

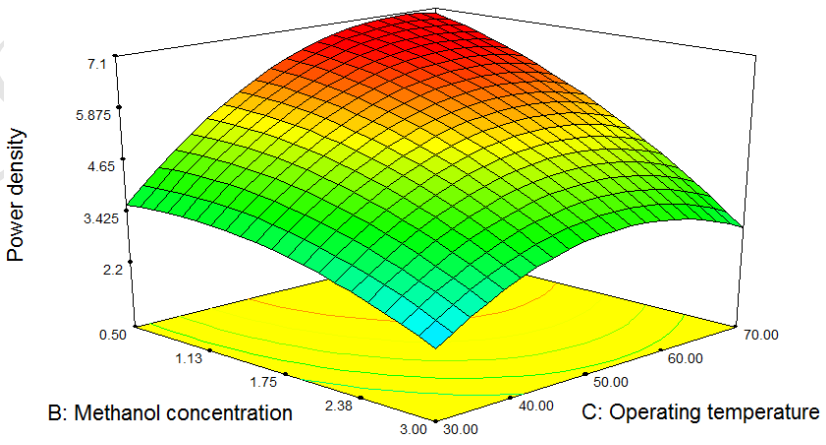

Figure 4 3D surface response of the relationship between methanol concentration and operating temperature with a power density at a methanol flow rate of 27.50 mL/min.

4.1.3 Effect of methanol concentration

The effect of methanol concentration on the power density is displayed shows in Figure 5. When measured at the operating temperature of 50°C, and the same flow rate, it was found that raising the concentration of methanol from 0.5 to 3 M would lower the power density significantly due to the greater crossover of methanol from the anode to the cathode (Chen et al., 2010). A high concentration gradient resulted in faster and greater fuel flow rate passing through the membrane (Calabriso et al., 2015; Prapainainar et al., 2015). The methanol that passed through the membrane generated excessive reversed current. It resulted in a drop in voltage and greatly reduced power density. And it was clearly seen that, the changing of methanol concentration had a greater effect on the power density compared to the methanol flow rate.

4.1.4 Effect of methanol flow rate

The effect of methanol flow rate on the fuel cell performance is shown in Figure 6. It is plotted between the methanol flow rate and operating temperature on the power density at a constant methanol concentration of 1.75 molar. Considering at the same operating temperature, raising the methanol flow rate from 5 ml/min gradually increased power density until the methanol flow rate was approximately 27.5 ml/min. After that, the power density started falling. A higher flow rate led to an increase in the mass transfer of fuel through the membrane, although, a higher fuel flow rate caused higher fuel cell efficiency during 5-27.5 ml/min due to high fuel transportation rate to the surface of the catalyst that was not a lack of fuel (Alipour Najmi et al., 2016). On the other hand, at too high a methanol flow rate, the power density dropped due to the greater volume of methanol diffused through the membranes. A methanol flow rate higher than 27.5 ml/min did not increase the power density but only removed CO_2 gas bubbles from

fuel cell flow channels and caused methanol transported to the active surface of catalyst efficiently. From Figure 6, at a flow rate higher than 27.5 ml/min, the performance should increase due to the greater methanol transportation rate to the catalyst. However, with increased methanol crossover that had a higher influence when the fuel flow rate was raised, the efficiency decreased. This was consistent with the research of Taymaz et al. (2011), Alzate et al. (2011), and Liu et al. (2011). Consequently, from Figure 6, it was noticeable that the operating temperature had a greater impact on the response than the methanol flow rate had.

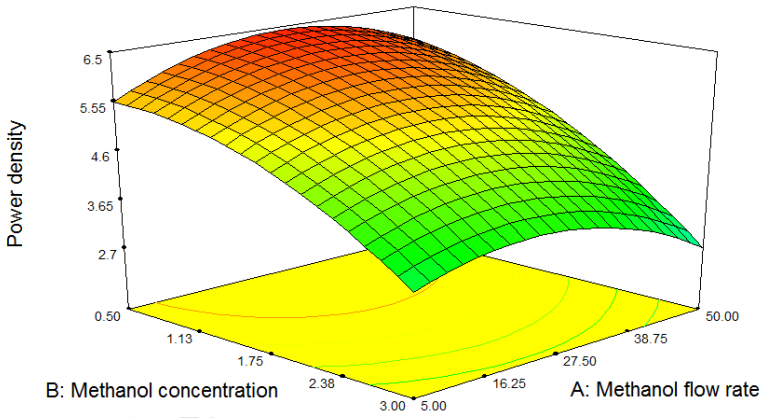

Figure 5 3D surface response of the relationship between methanol flow rate and methanol concentration with a power density at operating temperature of 50°C.

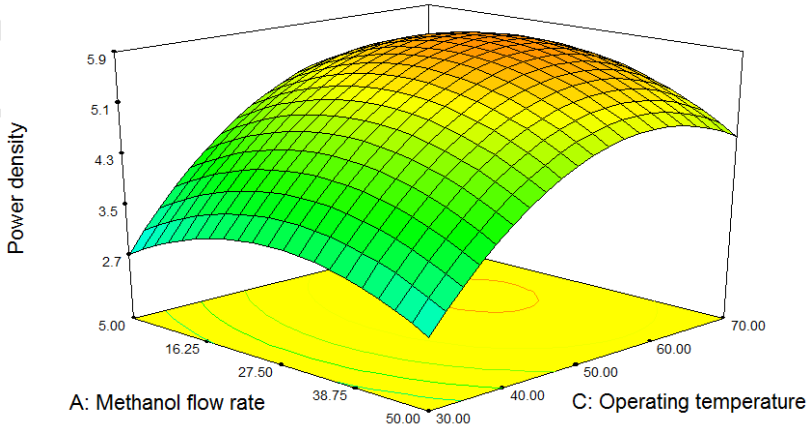

Figure 6 3D surface response of the relationship between methanol flow rate and operating temperature with a power density at methanol concentration of 1.75 M.

The optimum operating condition that maximized the power density was calculated by numerical method and set goal which is power density to maximize than the program generate the optimal condition. From the program, the operating conditions at 24.0 ml/min of methanol flow rate, 0.5 M of methanol concentration, and an operating temperature of 66.9°C generated the maximum power density (7.016 mW/cm^2). After adjusting to the optimum conditions according to the program, the actual power density from the single cell performance test was equal to 7.09 mW/cm^2, which was very close to the predicted value (only 1.04 % error). Therefore, it was concluded that the response surface was an accurate and reliable method to determine the optimum operating conditions for DMFC.

4.2 The optimization of direct ethanol fuel cell

This section shows the optimization of DEFC. The experiment and analysis was identical to those in the DMFC section. The operating conditions of DEFC obtained from RSM and the power density are provided in Table 3 and the statistical data from the analysis is shown in Table 4.

Table 3 Operating conditions of DEFC obtained from Design Expert 7.0 and power density from experiment.

Run	Ethanol flow rate (mL/min)	Ethanol conc. (M.)	Operating temperature. (°C)	Power density (mW/cm^2)
1	50.0	3.00	30	0.96
2	27.5	1.75	74	1.24
3	27.5	0.25	50	0.84
4	50.0	0.50	70	1.27
5	0.5	1.75	50	0.92

Run	Ethanol flow rate (mL/min)	Ethanol conc. (M.)	Operating temperature. (°C)	Power density (mW/cm^2)
6	50.0	3.00	70	0.85
7	27.5	1.75	50	1.1
8	5.0	0.50	70	1.79
9	5.0	3.00	30	0.72
10	5.0	3.00	70	1.12
11	5.0	3.00	70	1.06
12	5.0	0.50	30	0.85
13	5.0	3.00	30	0.72
14	50.0	3.00	70	0.83
15	54.5	1.75	50	1.03
16	27.5	1.75	74	1.31
17	50.0	0.50	30	0.82
18	50.0	3.00	30	0.86
19	27.5	0.25	50	0.8
20	5.0	0.50	30	0.82
21	27.5	3.25	50	0.64
22	27.5	1.75	50	1.16
23	27.5	1.75	26	0.47
24	50.0	3.00	30	0.96
25	27.5	1.75	74	1.24
26	27.5	1.75	26	0.44
27	27.5	3.25	50	0.71
28	50.0	0.50	30	0.87
29	54.5	1.75	50	1.03
30	5.0	0.50	70	1.83

Table 4 ANOVA results of DEFC for the response from the quadratic equation of Design Expert 7.0.

Source	Sum of Squares	df	Mean Square	F Value	p-value Prob> F
Model	2.52	9	0.28	15.61	<0.0001
A-Ethanol flow rate	0.06	1	0.06	3.34	0.0824
B-Ethanol concentration	0.34	1	0.34	19.23	0.0003
C-Cell temperature	1.32	1	1.32	73.63	< 0.0001
AB	0.06	1	0.06	3.15	0.0912
AC	0.25	1	0.25	13.81	0.0014
BC	0.30	1	0.30	16.73	0.0060
A^2	0.16	1	0.16	8.97	0.0071
B^2	0.02	1	0.02	1.27	0.2735
C^2	7.600E-003	1	7.600E-003	0.42	0.5223
Residual	0.40	20	0.02		
Pure Error	0.03	15	2.247E-003		
Cor Total	2.90	29			
Std. Dev.	0.13				
R-Squared	0.88				
Adj R-Squared	0.82				

4.2.1 Statistical analysis

The power density at any operating point of the DEFC was calculated using a model from equation (9). From the analysis of the variance (ANOVA) in Table 4, it was found that R-square and Adj R-Squared were equal to 0.8754 and 0.8193, respectively. It was concluded that the values were sufficiently high and the obtained equation served as an adequately accurate model for the prediction of the power density. The P-value of the model was less than 0.0001 (less than 0.05 level of significance). Thus it also proved that this model was reliable. It can also be observed that only the P-value of A was greater than 0.05, and this again demonstrated that the ethanol flow rate did not significantly affect the response (power density). The P-values of B and C were less than 0.05, which

indicated significant contributions to the power density similar to the DMFC case. Although the ethanol flow rate alone did not have a significant effect on the response, the P-value of the interaction effects between A and C, which was lower than 0.05, indicated that the effect of C (the temperature) significantly depended on the flow rate. The P-value of BC was also under the significance level, indicating that the ethanol concentration and the temperature interacted with each other. The P-values of squared effects, B^2 and C^2, were all greater than 0.05, and this indicated that their effects on the power density tended to be linear.

$$\text{Power Density} = 0.9-0.052A-0.13B+0.25C+0.059AB-0.12AC-0.14BC+0.14A^2-0.052B^2+0.03C^2 \quad (9)$$

where A is the ethanol flow rate (mL/min), B is the ethanol concentration (molar) and C is the operating temperature (°C).

The relationship between power density of DEFC obtained from the experiment and that from the program prediction is shown in Figure 7. It was observed that the power density from the experiment (point) was closer to that from the prediction model (line). It was suggested that the model was reliable. Figure 8 shows the plot between the residuals and the predicted value of the power density. It was found that the residuals were inclined to approach the x-axis and all of the investigated residual values were not greater than +3 or less than –3. This meant that the results from the model and the experiment were considered satisfactory.

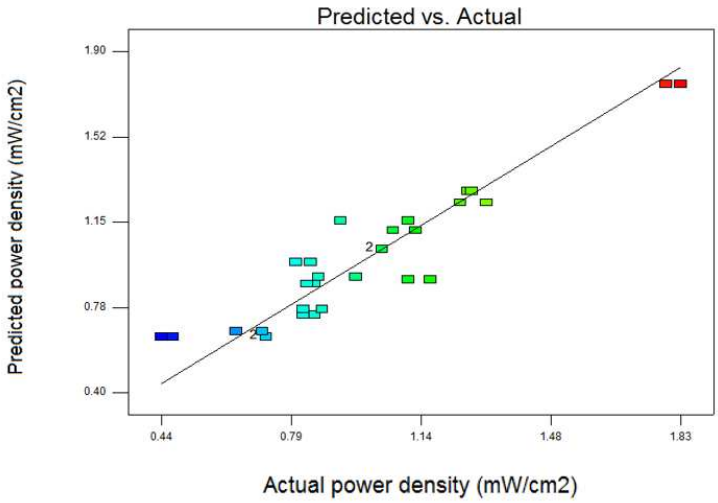

Figure 7 Maximum power density of DEFC between actual and predicted value.

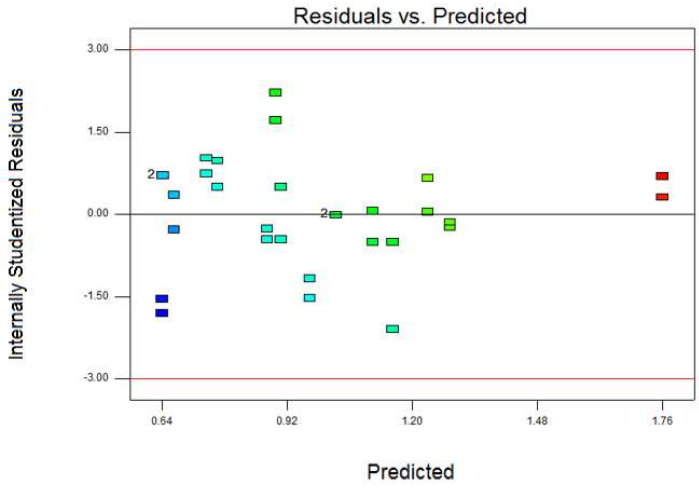

Figure 8 Residual value of power density and predicted power density of DEFC.

4.2.2 Effect of ethanol flow rate

Figure 9 presents the response plot between the ethanol flow rate and operating temperature on the power density. Regarding the concentration of ethanol at 0.5 M, it was

found that the power density was nearly flat when the ethanol flow rate increased. However, due to a significance of the interaction effect between the flow rate and the temperature, the change in power density when the operating temperature rose at an ethanol flow rate of 5 ml/min was higher than that at an ethanol flow rate of 50 ml/min. This was different from the DMFC in section 4.1 (Figure 6), which showed that varying levels of the flow rate did not change the relationship between the temperature and the power density.

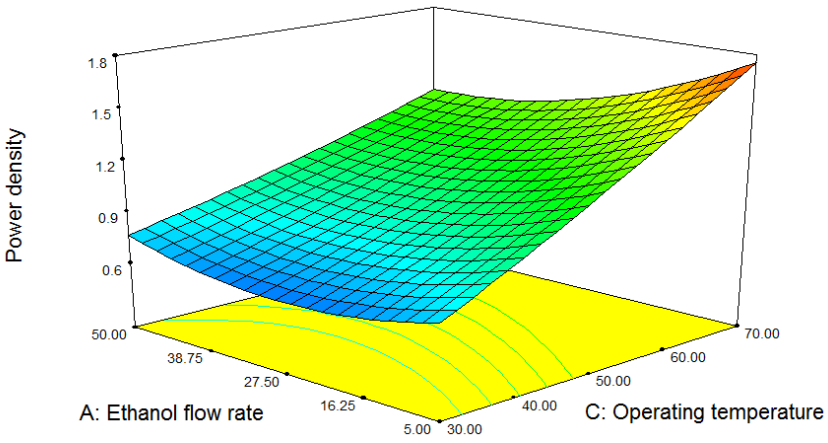

Figure 9 3D surface response of the relationship between ethanol flow rate and operating temperature with a power density at ethanol concentration of 0.5 M for DEFC.

4.2.3 The effect of ethanol concentration

Figure 10 shows the effect of ethanol concentration by surface plot between the concentration and the flow rate at the highest operating temperature of 70°C. At the same ethanol flow rate, increasing the ethanol concentration resulted in a gradual reduction in power density due to higher ethanol crossover (Assumpção et al., 2014). Figure 11 shows the effect of the ethanol concentration and operating temperature on the power density. It was found that the ethanol concentration had a powerful effect on the power density at the high temperature due to a high rate of ethanol diffusion.

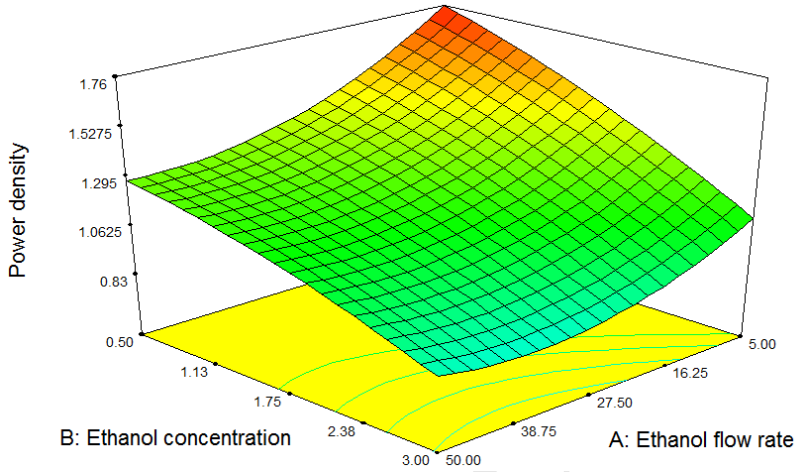

Figure 10 3D surface response of the relationship between ethanol concentration and ethanol flow rate with a power density at operating temperature70°C for DEFC.

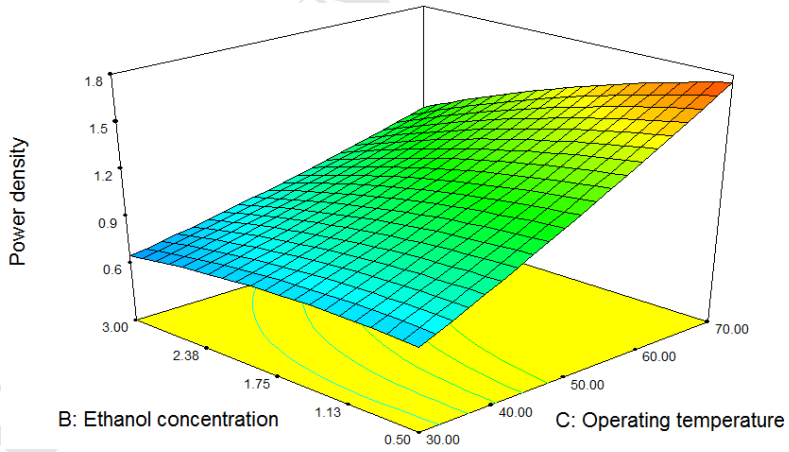

Figure 11 3D surface response of the relationship between ethanol concentration and operating temperature with a power density at ethanol flow rate 5 ml/min for DEFC.

4.2.4 The effect of operating temperature

Figure 12 shows the surface response between the ethanol concentration and operating temperature at 3 M. Considering a flow rate of 5 ml/min, the power density

increased when the operating temperature was raised. It was the same as that in DMFC and was consistent with research by Song et al. (2005). However, at a high ethanol flow rate of 50 ml/min, the power density didn't exhibit the same trend as that at a low flow rate. At a high ethanol concentration, high ethanol flow rate, and high operating temperature, the membrane had a high degree of swelling and a high order of ethanol crossover. A high temperature especially made the membrane structure expand due to softening of the fluorinated chain in the Nafion structure, as mentioned in section 4.1.2. Hence, the power density dropped, as seen in the Figure 12. The effect of the alcohol concentration on the power density in DEFC was less than that in DMFC, as seen in Figure 4 and 5.

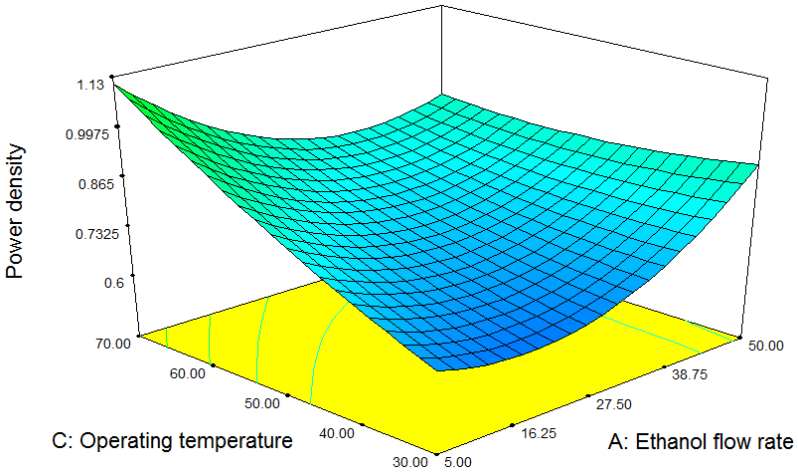

Figure 12 3D surface response of the relationship between operating temperature and ethanol flow rate with a power density at ethanol concentration 3 M for DEFC.

The optimization of DEFC that maximized the power density for the operating conditions was at an ethanol flow rate of 5 ml/min, ethanol concentration of 0.45 M, and operating temperature of 70°C. The model predicted the power density of 1.79 mW/cm^2 while that from the experiment at the same conditions was 1.78 mW/cm^2, which had only 1.107% error. In conclusion, DMFC demonstrated a higher performance than DEFC due

to the ease of oxidization of methanol compared to ethanol, which has a larger molecular size. Therefore, DMFC was selected to continue in the next section to discover the optimum MOR content in the Nafion composite membrane to reduce the alcohol crossover.

4.3 Effect of MOR content in Nafion-composite membrane on power density

This section aimed to modify the pristine Nafion membrane by using MOR to improve the performance by decreasing the fuel diffusion through the membrane. The variables to be studied were 0-10 wt% MOR, 1-8 M methanol and 30-70°C operating temperature. DMFC was focused on, because it provided a higher power density than DEFC as shown in the previous section. In this section, RSM with a historical method was used with three operating variables; methanol concentration, operating temperature and MOR content. The total experiment consist of 100 iterations. From section 4.1 and 4.2, the methanol flow rate was found not to have a significant effect on the maximum power density. Thus, it was removed from the independent variables in this section. The flow rate was fixed constant at 5 ml/min. The total data from the experiment are shown in Table 5.

4.3.1 Statistical analysis

The predicted model (Cubic model) is shows displayed in equation (10). From the ANOVA result in Table 6, it was found that the prediction model matched with the experimental data and a high precision of R-Square equal to 0.9460 was obtained. The P-values of all variables; ethanol concentration, operating temperature, and MOR content were lower than 0.05, which meant that all variables significantly affected the response. Figure 13 and 14 showed the high accuracy of power density from the experiment compared to that from the predicted model.

$$\text{Power Density} = 15.25-17.51A+6.69B-7.53C-6.52AB+1.23AC-2.29BC-0.19A^2-1.16B^2-1.82C^2+1.87ABC+1.32A^2B+0.23A^2C-1.59AB^2+1.23AC^2+0.061B^2C-1.28BC^2+11.89A^3-1.2B^3+4.28C^3 \quad (10)$$

where A is methanol concentration, B is operating temperature and C is MOR content in Nafion-composite membrane.

4.3.2 Effect of MOR content on power density

The effect of MOR content and operating temperature on the power density is presented in Figure 15 at a methanol concentration of 4.5 M. At a low operating temperature, the result showed that the increased MOR content improved the power density clearly until the MOR content was up to around 2.5 wt%. After that, the power density dropped. A too high MOR content caused the proton conductivity of membrane to fall, because protons from the methanol oxidation diffused through the membrane with more difficulty. This resulted in a slow rate of reduction leading to the performance reduction. This was in agreement with Li (2007) that when zeolite-A loading in the Nafion membrane was increased from 5 to 15 wt%, the methanol permeability decreased from 2.3×10^{-6} cm^2/s to around $1\times10^{-6}cm^2/s$ leading to the worsening performance. However, it also reduced the proton conductivity from 0.6 $S\cdot m^{-1}$ to 0.2 $S\cdot m^{-1}$. Thus, they concluded that a high content of inorganic filler did not improve the methanol resistance.

At a high temperature, the result of the MOR content on the power density displayed the same tendency as that at a low temperature. Increasing the MOR content reduced the methanol permeability which may be due to separation of MOR particles in the membrane and formed a MOR layer at the bottom of the mold during the recast process. Increasing the MOR loading, the layer became thicker while the polymer layer became thinner and the total thickness of the membrane also increased. This non-uniform dispersion of the MOR content and 2-layer-form in the Nafion membrane caused proton permeability to decrease, because the MOR layer acted as a barrier that blocked proton

diffusion as well as methanol diffusion. Hence, only a small amount of MOR was needed for the highest power density.

Table 5 Maximum power density at each condition of DMFC with MOR content.

Run	Methanol conc. (M)	Temperature (°C)	MOR content (wt%)	Power density (mW/cm^2)
1	1	30	0	9.481
2	1	30	3	9.156
3	1	30	5	8.889
4	1	30	7.5	6.291
5	1	30	10	7.398
6	1	40	0	14.588
7	1	40	3	14.459
8	1	40	5	14.163
9	1	40	7.5	9.728
10	1	40	10	10.716
11	1	50	0	21.333
12	1	50	3	20.711
13	1	50	5	22.202
14	1	50	7.5	14.519
15	1	50	10	13.926
16	1	60	0	29.116
17	1	60	3	27.595
18	1	60	5	30.528
19	1	60	7.5	19.99
20	1	60	10	18.39
21	1	70	0	37.886
22	1	70	3	34.844
23	1	70	5	40.741
24	1	70	7.5	23.644
25	1	70	10	22.311

Run	Methanol conc. (M)	Temperature (°C)	MOR content (wt%)	Power density (mW/cm^2)
26	2	30	0	10.43
27	2	30	3	11.022
28	2	30	5	12.069
29	2	30	7.5	9.728
30	2	30	10	8.711
31	2	40	0	16.622
32	2	40	3	16.978
33	2	40	5	17.6
34	2	40	7.5	13.758
35	2	40	10	12.207
36	2	50	0	25.126
37	2	50	3	23.941
38	2	50	5	25.481
39	2	50	7.5	17.699
40	2	50	10	16.514
41	2	60	0	34.607
42	2	60	3	31.526
43	2	60	5	33.333
44	2	60	7.5	22.025
45	2	60	10	20.444
46	2	70	0	41.64
47	2	70	3	37.294
48	2	70	5	38.449
49	2	70	7.5	24.444
50	2	70	10	25.857

Run	Methanol conc. (M)	Temperature (°C)	MOR content (wt%)	Power density (mW/cm^2)
51	4	30	0	9.886
52	4	30	3	9.565
53	4	30	5	13.037
54	4	30	7.5	7.511
55	4	30	10	8.346
56	4	40	0	14.815
57	4	40	3	14.667
58	4	40	5	18.578
59	4	40	7.5	10.252
60	4	40	10	11.2
61	4	50	0	19.23
62	4	50	3	19.881
63	4	50	5	23.585
64	4	50	7.5	12.444
65	4	50	10	13.274
66	4	60	0	22.163
67	4	60	3	23.141
68	4	60	5	27.931
69	4	60	7.5	13.274
70	4	60	10	13.965
71	4	70	0	21.57
72	4	70	3	25.126
73	4	70	5	25.679
74	4	70	7.5	12.978
75	4	70	10	12.444
76	8	30	0	8.217
77	8	30	3	8.059
78	8	30	5	7.388
79	8	30	7.5	4.84
80	8	30	10	5.926
81	8	40	0	10.44
82	8	40	3	9.659
83	8	40	5	8.711
84	8	40	7.5	5.373
85	8	40	10	6.281
86	8	50	0	11.062
87	8	50	3	10.193
88	8	50	5	8.919
89	8	50	7.5	5.965
90	8	50	10	6.519
91	8	60	0	10.904
92	8	60	3	10.232
93	8	60	5	8.642
94	8	60	7.5	5.847
95	8	60	10	6.173
96	8	70	0	8.533
97	8	70	3	8.612
98	8	70	5	6.519
99	8	70	7.5	4.691
100	8	70	10	4.889

Table 6 ANOVA results for the cubic equation of Design Expert 7.0.

Source	Sum of squares	df	Mean square	F-value	P-value
Model	7934.051	19	417.5816	73.71489	< 0.0001
A-Ethanol flowrate	392.5173	1	392.5173	69.29033	< 0.0001
B-Ethanol concentration	172.6258	1	172.6258	30.47331	< 0.0001
C-Cell temperature	199.0803	1	199.0803	35.14328	< 0.0001
AB	1221.249	1	1221.249	215.5848	< 0.0001
AC	41.6369	1	41.6369	7.350084	0.0082
BC	117.1854	1	117.1854	20.68652	< 0.0001
A^2	0.423932	1	0.423932	0.074836	0.7851
B^2	21.92754	1	21.92754	3.870827	0.0526
C^2	56.86136	1	56.86136	10.03763	0.0022
ABC	49.48993	1	49.48993	8.736363	0.0041
A^2B	14.11684	1	14.11684	2.492019	0.1184
A^2C	0.397844	1	0.397844	0.070231	0.7917
AB^2	25.94392	1	25.94392	4.579831	0.0354
AC^2	16.34981	1	16.34981	2.886201	0.0932
B^2C	0.031471	1	0.031471	0.005555	0.9408
BC^2	15.26076	1	15.26076	2.693954	0.1047
A^3	175.1348	1	175.1348	30.91622	< 0.0001
B^3	6.430057	1	6.430057	1.135086	0.2899
C^3	76.99257	1	76.99257	13.59135	0.0004
Residual	453.1856	80			
Cor Total	8387.236	99			
Std. Dev.	2.39				
R-Squared	0.9460				
Adj R-Squared	0.9331				

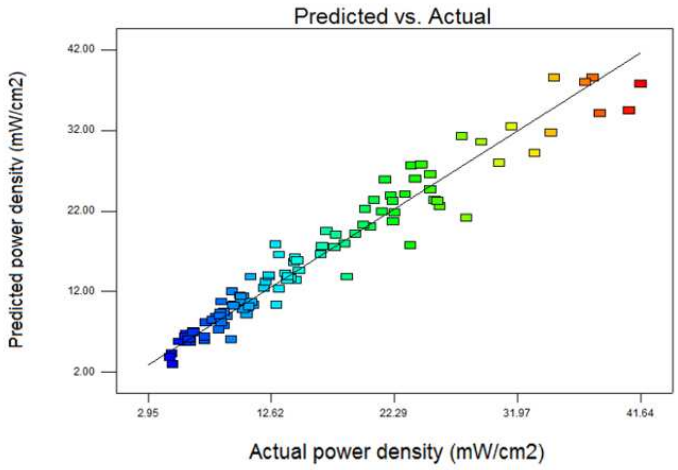

Figure 13 Maximum power density of DMFC between actual and predicted values (membrane with MOR).

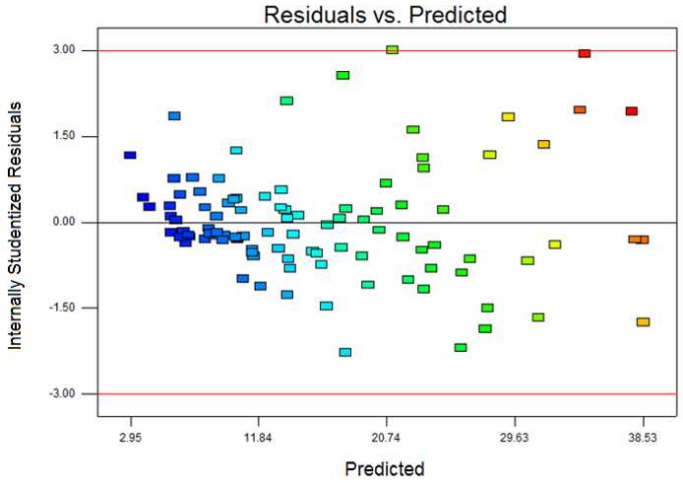

Figure 14 Residual value of power density and predicted power density of DMFC (membrane with MOR).

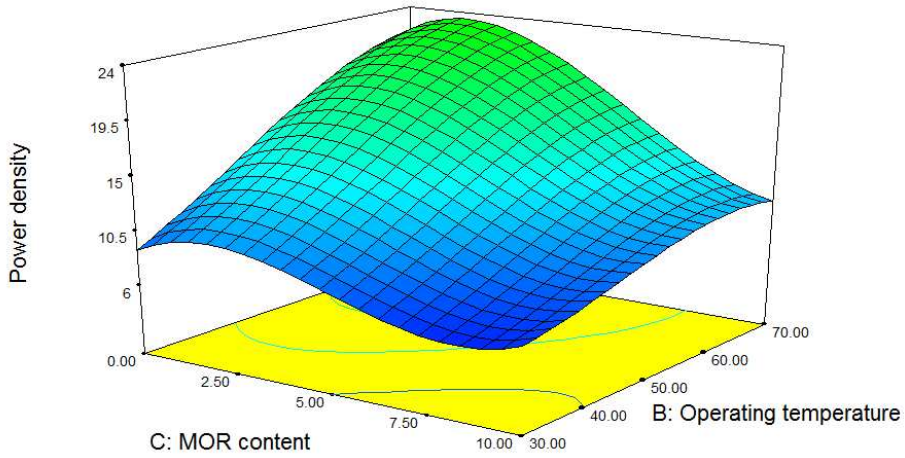

Figure 15 3D surface response of the relationship between MOR content and operating temperature with the power density at methanol concentration 4.5 M.

4.3.3 Effect of methanol concentration on power density

Figure 16 shows the surface response between the methanol concentration and the MOR content at an operating temperature of 70°C. It was found that the power density decreased when the methanol concentration increased from 1 M to 8 M. This was similar to that in section 4.1 and 4.2. The greater alcohol permeability was found when its concentration was raised. It was also found that the concentration of methanol had a more significant effect on the power density than MOR content was, as seen in Figure 16.

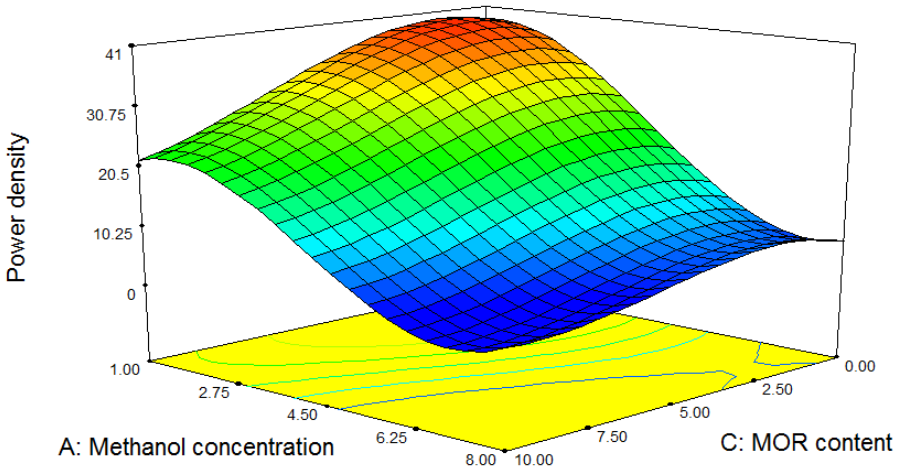

Figure 16 3D surface response of the relationship between methanol concentration and MOR content with a power density at an operating temperature of 70°C.

4.3.4 Effect of temperature on the power density

The effect of the methanol concentration and operating temperature on the power density at 1 M is shown in Figure 17. It was found that the power density continued increasing when the operating temperature increased. The maximum power density was at the highest operating temperature with a MOR content of around 2.5 wt%.

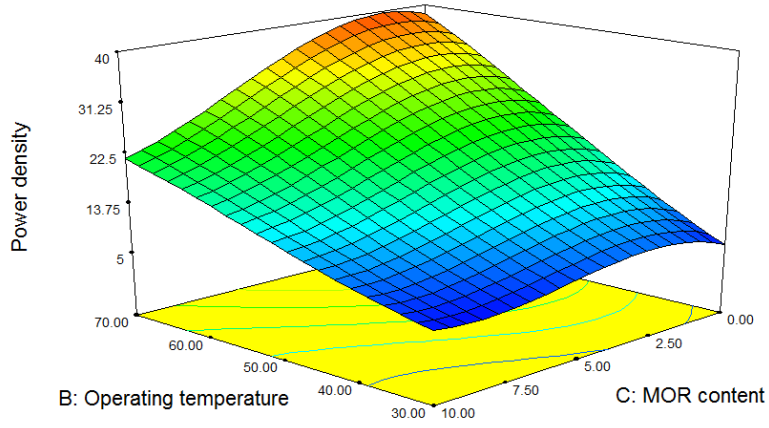

Figure 17 3D surface response of the relationship between operating temperature and MOR content with a power density at a methanol concentration of 1 M.

The optimization by the response surface to maximizing the power density from the predicted model in equation (10) indicated that the power density at a methanol concentration of 1.35 M, operating temperature of 70°C, and MOR content of 1.47 wt% was maximum (40.012 mW/cm^2), which is provided in Figure 18. The value increased from that of the membrane without MOR by around 3.22% when compared to the predicted power density at the same conditions of methanol concentration and operating temperature at 0 wt% of MOR content (38.7627 mW/cm^2).

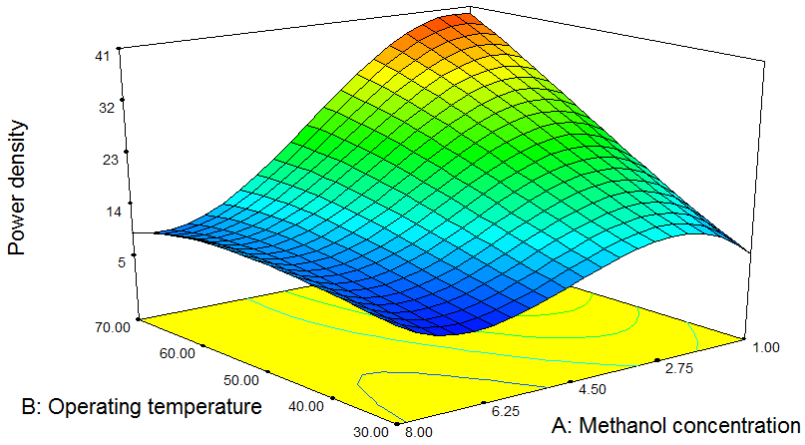

Figure 18 3D surface response of the relationship between operating temperature and methanol concentration with a power density at a MOR content 1.47 wt%.

The electricity production of DAFC releases CO_2 which is a by-product of the reaction with the atmosphere. Finding the most optimal conditions then becomes extremely important in order to have a minimum amount of CO_2 while obtaining the highest power density per unit of fuel. Operating fuel cells at the optimum conditions is worth as much as the same amount of fuel used at other conditions. For example, when DMFC is operated at 30°C with a methanol concentration of 4 M, methanol flow rate of 5 ml/min, and MOR content of 0 wt%, the power density obtained is equal to 9.886 mW/cm^2. This releases CO_2 176 g/liter of fuel. If the optimum condition is set (methanol concentration of 1.35 M, operating temperature of 70°C, and MOR content of 1.47 wt%)

the power density of 40.012 mW/cm^2 is obtained. At this condition, the release of CO_2 is only 59.4 g/liter of fuel. The obtained power density divided by weight of CO_2 released of that condition and the optimum condition are equal to 0.056 and 0.673, respectively. This represents a 12-fold increase. It can be seen that operating the fuel cell at the optimal conditions is the way to use resources wisely (lower CO_2 emission) and to maximize energy (power density). Therefore, this method is important towards a green and cleaner energy production.

5. Conclusion

This study employed the design of experiment (the central composite design) and the response surface methodology to find the optimum conditions of DMFC and DEFC. The conditions to be optimized were methanol flow rate, alcohol concentration, and operating temperature on the power density which represented the fuel cell performance. The result showed that the operating temperature and alcohol concentration had a significant impact on the power density, while the effect of the alcohol flow rate on the power density was not significant. In DMFC, by using the quadratic model to optimize the operating conditions, it was found that the optimum point was at a methanol flow rate of 24.0 ml/min, methanol concentration of 0.5 molar and operating temperature of 66.9°C. The maximum power density predicted from the model was equal to 7.016 mW/cm^2, while the actual maximum power density was 7.09 mW/cm^2 (only 1.04 % error). In case of DEFC, the optimum was at an ethanol flow rate of 5 ml/min, ethanol concentration of 0.45 M and operating temperature of 70°C. The power density predicted was equal to 1.79 mW/cm^2. R-square values of the two models were 0.94 and 0.88 for DMFC and DEFC, respectively. Therefore, it was concluded that RSM was a very suitable and reliable method to determine the optimum operating conditions of DMFC and DEFC. Adding MOR in the Nafion membrane to from a Nafion-composite membrane was also designed to improve the performance of DMFC. The results showed that the power density of the fuel cell was improved when adding a small amount of

MOR. The optimum conditions from RSM were at a methanol concentration of 1.35 M, operating temperature of 70°C and MOR content of 1.47 wt%, which led to a power density of 40.012 mW/cm^2. From this study, it was concluded that the optimization of the operating conditions was were important to obtain the optimum energy or to allow the fuel cell to work in high efficiency mode. It is an effective way to achieve greener and cleaner production of energy.

6. ACKNOWLEDGMENT

The authors would like to gratefully acknowledge the Thailand Research Fund (TRF) for funding the project TRG5780256. The funding was also provided by Kasetsart University's Research Development Institute (KURDI), the Faculty of Engineer, Kasetsart University, Faculty of Engineering, KMUTNB, and the Faculty of Engineering, KhonKaen University.

7. Reference

Abdullah, S., Kamarudin, S.K., Hasran, U.A., Masdar, M.S., Daud, W.R.W., 2015. Development of a conceptual design model of a direct ethanol fuel cell (DEFC). International Journal of Hydrogen Energy 40, 11943-11948.

Alipour Najmi, A., Rowshanzamir, S., Parnian, M.J., 2016. Investigation of NaOH concentration effect in injected fuel on the performance of passive direct methanol alkaline fuel cell with modified cation exchange membrane. Energy 94, 589-599.

Alshehria, A.N.Z., Ghanem, K.M., Al-Garni, S.M., 2015. Application of a five level central composite design to optimize operating conditions for electricity generation in a microbial fuel cell. Journal of Taibah University for Science.

Alzate, V., Fatih, K., Wang, H., 2011. Effect of operating parameters and anode diffusion layer on the direct ethanol fuel cell performance. Journal of Power Sources 196, 10625-10631.

Andreasen, K.P., Sovacool, B.K., 2015. Hydrogen technological innovation systems in practice: comparing Danish and American approaches to fuel cell development. Journal of Cleaner Production 94, 359-368.

Assumpção, M.H.M.T., Nandenha, J., Buzzo, G.S., Silva, J.C.M., Spinacé, E.V., Neto, A.O., De Souza, R.F.B., 2014. The effect of ethanol concentration on the direct ethanol fuel cell performance and products distribution: A study using a single fuel cell/attenuated total reflectance – Fourier transform infrared spectroscopy. Journal of Power Sources 253, 392-396.

Badwal, S.P.S., Giddey, S., Kulkarni, A., Goel, J., Basu, S., 2015. Direct ethanol fuel cells for transport and stationary applications – A comprehensive review. Applied Energy 145, 80-103.
Calabriso, A., Cedola, L., Del Zotto, L., Rispoli, F., Santori, S.G., 2015. Performance investigation of Passive Direct Methanol Fuel Cell in different structural configurations. Journal of Cleaner Production 88, 23-28.
Chen, S., Ye, F., Lin, W., 2010. Effect of operating conditions on the performance of a direct methanol fuel cell with PtRuMo/CNTs as anode catalyst. International Journal of Hydrogen Energy 35, 8225-8233.
Cheng, Y., Shen, P.K., Saunders, M., Jiang, S.P., 2015. Core–Shell Structured PtRuCox Nanoparticles on Carbon Nanotubes as Highly Active and Durable Electrocatalysts for Direct Methanol Fuel Cells. Electrochimica Acta 177, 217-226.
Hall, J., Kerr, R., 2003. Innovation dynamics and environmental technologies: the emergence of fuel cell technology. Journal of Cleaner Production 11, 459-471.
Heysiattalab, S., Shakeri, M., Safari, M., Keikha, M.M., 2011. Investigation of key parameters influence on performance of direct ethanol fuel cell (DEFC). Journal of Industrial and Engineering Chemistry 17, 727-729.
Jurzinsky, T., Bär, R., Cremers, C., Tübke, J., Elsner, P., 2015. Highly active carbon supported palladium-rhodium PdXRh/C catalysts for methanol electrooxidation in alkaline media and their performance in anion exchange direct methanol fuel cells (AEM-DMFCs). Electrochimica Acta 176, 1191-1201.
Kahveci, E.E., Taymaz, I., 2014. Experimental investigation on water and heat management in a PEM fuel cell using response surface methodology. International Journal of Hydrogen Energy 39, 10655-10663.
Lecksiwilai, N., Gheewala, S.H., Sagisaka, M., Yamaguchi, K., Net Energy Ratio and Life cycle greenhouse gases (GHG) assessment of bio-dimethyl ether (DME) produced from various agricultural residues in Thailand. Journal of Cleaner Production.
Li, X., 2007. Development of Composite Membranes for Direct Methanol Fuel Cell, in School of Chemical Engineering and Analytical Science, The University of Manchester: Manchester, p. 243.
Li, Y., Liu, C., Liu, Y., Feng, B., Li, L., Pan, H., Kellogg, W., Higgins, D., Wu, G., 2015. Sn-doped TiO2 modified carbon to support Pt anode catalysts for direct methanol fuel cells. Journal of Power Sources 286, 354-361.
Liu, C.-W., Chang, Y.-W., Wei, Y.-C., Wang, K.-W., 2011. The effect of oxygen containing species on the catalytic activity of ethanol oxidation for PtRuSn/C catalysts. Electrochimica Acta 56, 2574-2581.
Mallick, R.K., Thombre, S.B., Shrivastava, N.K., 2015. A critical review of the current collector for passive direct methanol fuel cells. Journal of Power Sources 285, 510-529.
Mudiraj, S.P., Biswas, M.A.R., Lear, W.E., Crisalle, O.D., 2015. Comprehensive mass transport modeling technique for the cathode side of an open-cathode direct methanol fuel cell. International Journal of Hydrogen Energy 40, 8137-8159.
Okur, O., Alper, E., Almansoori, A., 2014. Optimization of catalyst preparation conditions for direct sodium borohydride fuel cell using response surface methodology. Energy 67, 97-105.
Permpool, N., Bonnet, S., Gheewala, S.H., Greenhouse gas emissions from land use change due to oil palm expansion in Thailand for biodiesel production. Journal of Cleaner Production.
Prapainainar, P., Theampetch, A., Kongkachuichay, P., Laosiripojana, N., Holmes, S.M., Prapainainar, C., 2015. Effect of solution casting temperature on properties of nafion composite

membrane with surface modified mordenite for direct methanol fuel cell. Surface and Coatings Technology 271, 63-73.
Sha Wang, L., Nan Lai, A., Xiao Lin, C., Gen Zhang, Q., Mei Zhu, A., Lin Liu, Q., 2015. Orderly sandwich-shaped graphene oxide/Nafion composite membranes for direct methanol fuel cells. Journal of Membrane Science 492, 58-66.
Song, S., Zhou, W., Tian, J., Cai, R., Sun, G., Xin, Q., Kontou, S., Tsiakaras, P., 2005. Ethanol crossover phenomena and its influence on the performance of DEFC. Journal of Power Sources 145, 266-271.
Taymaz, I., Akgun, F., Benli, M., 2011. Application of response surface methodology to optimize and investigate the effects of operating conditions on the performance of DMFC. Energy 36, 1155-1160.
Wu, C., Wu, J., Luo, H., Wang, S., Chen, T., 2016. Ultrasonic radiation to enable improvement of direct methanol fuel cell. Ultrasonics Sonochemistry 29, 363-370.
Yoonoo, C., Dawson, C.P., Roberts, E.P.L., Holmes, S.M., 2011. Nafion®/mordenite composite membranes for improved direct methanol fuel cell performance. Journal of Membrane Science 369, 367-374.
Yuan, Z., Yang, J., Zhang, Y., Zhang, X., 2015. The optimization of air-breathing micro direct methanol fuel cell using response surface method. Energy 80, 340-349.
Zainoodin, A.M., Kamarudin, S.K., Masdar, M.S., Daud, W.R.W., Mohamad, A.B., Sahari, J., 2015. Optimization of a porous carbon nanofiber layer for the membrane electrode assembly in DMFC. Energy Conversion and Management 101, 525-531.

Highlight

- Optimum operating condition was predicted using Response Surface Method.
- Operating temperature and alcohol concentration had great impact on power density.
- DMFC used composite membrane produced higher power than used pristine Nafion.